ChemComm

Chemical Communications

rsc.li/chemcomm

ROYAL SOCIETY
OF CHEMISTRY

COMMUNICATION
Yun-Bao Jiang *et al.*
Supramolecular helix of an oligomeric azapeptide building
block containing four β-turn structures

60 YEARS
ANNIVERSARY

COMMUNICATION

Check for updates

Supramolecular helix of an oligomeric azapeptide building block containing four β-turn structures†

Yingdan Zhao, [a] Xiaosheng Yan [ab] and Yun-Bao Jiang [*a]

Oligomers of benzoylalanine-based amidothioureas containing four β-turn structures spaced by *meta*-substituted benzenes were shown to undergo assembly in dilute CH₃CN solution into supramolecular helices of enhanced supramolecular helicity, whereas those spaced by *para*-substituted benzene spacer(s) or those spaced by *meta*-substituted benzenes but with one or two β-turns exhibit a substantially decreased tendency of assembling.

Helical structures such as the protein α-helix and DNA double helix are of great significance in life sciences. Scientists have thus been exploring the design and development of diverse biomimetic artificial helices of varying functionalities. Supramolecular helical structures have attracted considerable attention also because of their adaptable cavity size, processability, flexibility, and ease of modification and functionalization.[1] One strategy for constructing supramolecular helices is to elongate short building blocks in a helically folded conformation, through end-to-end noncovalent interactions.[1–4] Among them, aromatic foldamers of good predictability have been widely employed.[5–9] Those helices can be applied to the recognition, encapsulation and transport of a variety of ions and neutral molecules,[6,10–12] and the properties of the supramolecular helices can be altered by structural adjustments thus to achieve regulated selectivity and activity.[13,14]

Yet, the design of novel building blocks remains challenging. We have recently built single- and double-stranded supramolecular helices in the solid phase and in dilute solution, using a bis(*N*-amidothiourea) motif that contains two β-turns in the terminal or central parts of the molecule as the building block, such that the intermolecular halogen bonding bridges

molecules into helices.[15,16] With these short building blocks, their concentrations might need to be high to allow a long enough helix to be well characterized, which may become hard as their solubility could be a limiting factor. The minimal optimal number of turn structures and the way of their linkage shall then be critical for their successful assembly into supramolecular helices.

Reported herein are our efforts to achieve amidothiourea-based oligomeric building blocks that contain four β-turn structures spaced by *meta*-substituted benzenes, **1L** and **1D**, taking, respectively, L- and D-alanine as the chiral source (Fig. 1a and b). Two iodine atoms are introduced at the *para*-positions of the two terminal phenyl rings to possibly afford intermolecular halogen bonding. Experiments show that these two oligomeric compounds function to assemble into stable supramolecular helices in dilute CH₃CN solution, *via* halogen bonding. The *para*-substituted benzene-spaced counterparts do not assemble well (one of the four being *para*-substituted) or do not assemble at all (more than one) (**3L**, **4L** and **5L**, Fig. 1b), and those *meta*-substituted but containing one or two β-turns (**6L** and **7L**, Fig. 1b) do not assemble either.

The β-turn structure in *N*-amidothiourea derivatives provides helical fragments. ^{1}H NMR spectra show that with increasing solution temperature, the chemical shift of each –NH proton in **1L** moves downfield, at different rates (Fig. S1, ESI†). Notably, the resonance of the –NH[d] proton exhibits the smallest temperature coefficient ($\Delta\delta/\Delta T = -2.44$ ppb °C *versus* –NH[a]: -8.96, –NH[b]: -8.73 and –NH[c]: -8.76, Fig. 2a), indicating that it is less influenced by solution temperature. This means that it is protected, to some extent, agreeing with its taking part in an intramolecular hydrogen bond. Furthermore, the chemical shift of –NH[d] remains unchanged upon changing the volume ratio of DMSO-d_6 to CD₃CN in their binary mixtures (Fig. S2 and S3, ESI†), providing further evidence for the presence of the hydrogen bonded β-turn.

Repetition of the β-turn structure, due to its helical character, may facilitate the elongation of the oligomeric building block. This will result in a folding propensity of the formed

a Department of Chemistry, College of Chemistry and Chemical Engineering, the MOE Key Laboratory of Spectrochemical Analysis and Instrumentation, Xiamen University, Xiamen 361005, China. E-mail: ybjiang@xmu.edu.cn

b Fujian Provincial Key Laboratory of Innovative Drug Target Research and State Key Laboratory of Cellular Stress Biology, School of Pharmaceutical Sciences, Xiamen University, Xiamen, Fujian 361102, China

† Electronic supplementary information (ESI) available. See DOI: https://doi.org/10.1039/d3cc04859d
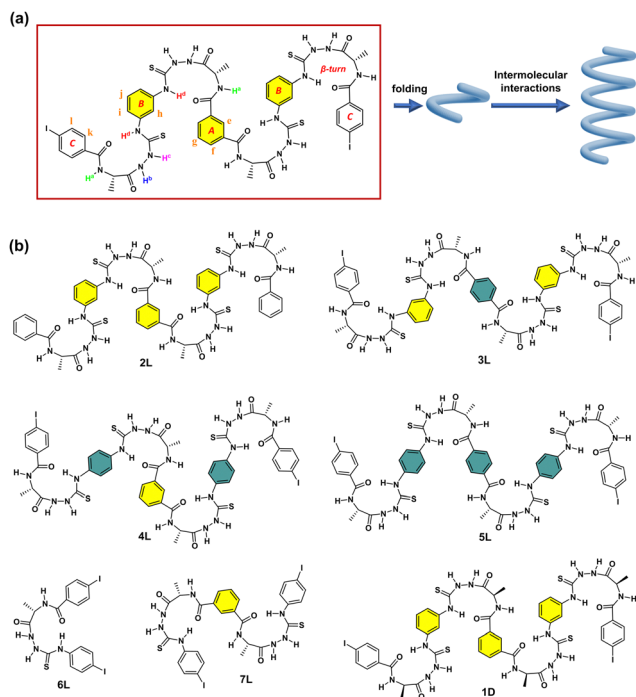
Fig. 1 (a) Chemical structure of **1L** with numbering of protons and schematic illustration of the formation of a supramolecular helix from the helical oligomer. (b) Chemical structures of control compounds **2L**, **3L**, **4L**, **5L**, **6L**, **7L** and **1D**.
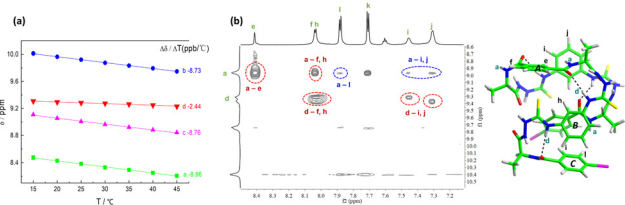

Fig. 2 (a) Influence of solution temperature on the resonance of the −NH protons of **1L** in 90:10 (v/v) CD_3CN/DMSO-d_6 mixture and the fitted temperature coefficients. (b) Expanded 2D NOESY spectrum of **1L** in DMSO-d_6 and DFT (M06-2X-D3/6-31G**)-optimized structure of **1L** in the gas phase. Dashed black lines highlight the intramolecular hydrogen bonds for the β-turns.

oligomer, indicated by the DFT-optimized structure of **1L** in the gas phase (Fig. 2b). The 2D NOESY spectrum of **1L** in DMSO-d_6 also reveals the folded conformation of **1L** (Fig. 2b and Fig. S4, ESI†). NOE coupling signals between H^a–H^e and H^a–H^f indicate that the β-turns on two sides of benzene ring **A** are oriented in opposite directions. Similarly, the β-turns on two sides of benzene ring **B** also exhibit different orientations, as evidenced by the NOE signals between H^d–H^h, H^d–H^i, and H^d–H^j. Furthermore, the NOE couplings between H^a–H^i/H^j and H^a–H^l further proved that **1L** is folded, which brings NH^a and benzene rings **B** and **C** into close proximity, in line with the calculated monomeric structure of **1L**.

1L in the folded conformation may facilitate its supramolecular assembly, as a basic building block. We did observe such
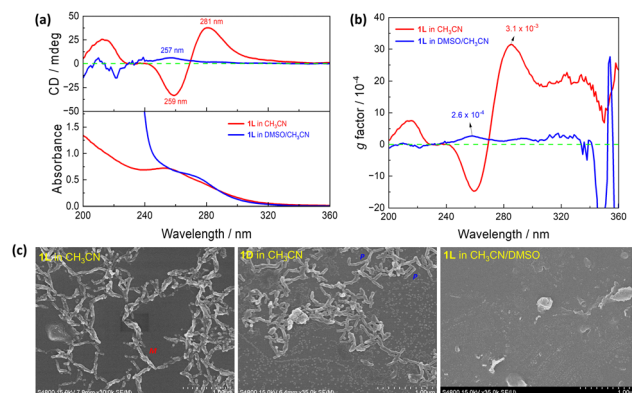

Fig. 3 (a) Absorption and CD spectra and (b) g-factor profiles of **1L** in CH_3CN and in 1:199 (v/v) DMSO/CH_3CN. Due to weak absorbance in the range of 320–360 nm, the g-factor profiles within this region exhibit significant fluctuations. (c) SEM images of air-dried samples of **1L** and **1D** in CH_3CN and **1L** in 1:199 (v/v) DMSO/CH_3CN on platinum-coated silicon wafers. [**1L**] = [**1D**] = 10 μM.

supramolecular assembly in CH_3CN. In DMSO, a highly polar aprotic solvent, assembly of it would thus be much less, if any. Experiments in both pure CH_3CN and DMSO/CH_3CN binary solvents were carried out in detail. In CH_3CN, the absorption spectrum of **1L** displays a band at 255 nm and a shoulder at 275 nm, accompanied by prominent Cotton effects at 281 nm, 259 nm, and 213 nm in the CD spectrum; in CH_3CN containing 0.5% DMSO by volume, however, only a faint CD signal at 257 nm was observed (Fig. 3a). Furthermore, the anisotropic factor, g, in CH_3CN (3.1×10^{-3}, Fig. 3b) is significantly higher, *ca.* 12 times that in DMSO/CH_3CN (2.6×10^{-4}, Fig. 3b). Dynamic light scattering (DLS, Fig. S5, ESI†) allows access to the size distributions of **1L** in different solvents. The diameter of the **1L** at the same concentration in DMSO/CH_3CN was measured as 3.2 nm, whereas in CH_3CN it reached 22.8 nm. This further substantiates the assumption that **1L** forms assemblies in CH_3CN, whereas in DMSO/CH_3CN it remains as a monomer. Meanwhile, SEM images of air-dried samples from CH_3CN solutions of **1L** reveal the presence of ordered short *M*-helical assemblies and those of **1D** the *P*-helical structures, whereas no regular morphology is observed from the samples prepared in DMSO/CH_3CN (Fig. 3c). These findings provide compelling evidence that **1L** and **1D** assemble into supramolecular helices in CH_3CN.

Supramolecular assembly occurs when the dimensionless concentration exceeds unity ($c_T K_e > 1$), where c_T represents the total concentration and K_e refers to the equilibrium constant. Hence, a critical concentration, corresponding to K_e^{-1}, is required for the helical assembly of **1L** to occur.[17] Indeed, CD signals of **1L** in CH_3CN measured at different concentrations indicate a remarkably low critical assembly concentration, *ca.* 1 μM (Fig. S6, ESI†), through which a high K_e value of 1.0×10^6 M^{-1} is estimated. Investigation into the concentration-dependent g factor of **1L** reveals an increase in g with increasing concentration from 1 to 5 μM (Fig. S7, ESI†) after which it levels off. However, at a concentration below 1 μM, the g factor varies

irregularly. Based on these observations, it is inferred that **1L** exhibits a state of assembly instability at concentrations close to or below the critical assembly concentration, that the monomer and aggregates may exchange rapidly. As the concentration increases beyond this critical concentration, the monomer molecules assemble to lead to helical chain extension, indicated by an increase in the g factor. As the concentration approaches 5 μM, the chain ceases to propagate, such that a stable assembly state is reached, which the g factor does not change any more. The concentration-dependent DLS data of **1L** in CH₃CN corroborate this pattern of variation in g factor (Fig. S8 *vs.* S7, ESI†). Consequently, it is concluded that the supramolecular helix of **1L** in CH₃CN possesses a finite size range, rather than an infinite extension.

According to our previous research,[15,16] it is assumed that the supramolecular helix of **1L** is probably driven by intermolecular halogen bonding. Thus, control compound **2L** (Fig. 1b), without I-substituents, was examined. First, in CH₃CN the CD intensity of **2L** is significantly weaker than that of **1L**, with no discernible CD signal associated with the assembly (Fig. S9, ESI†). Second, upon increasing the concentration of **2L**, no obvious changes were observed (Fig. S10, ESI†). Third, the g factor of **2L** reaches a maximum value of 3.1×10^{-4} at 244 nm (Fig. 4a and Fig. S11, ESI†), one tenth that of the maximum value of **1L** (3.1×10^{-3} at 285 nm). It is reasonable to conclude that **2L** is unable to assemble into supramolecular species in CH₃CN. Indeed, DLS experiments reveal that the diameters of **2L** in CH₃CN are around 3.3 nm (Fig. S12, ESI†), approximately 7 times smaller than those of **1L**. No assembly morphology was observed in the SEM images of **2L** (Fig. S13, ESI†). Taken together, it is concluded that control compound **2L** does not undergo assembly in CH₃CN, suggesting thus the role of I-substituents in **1L** in driving its assembly into supramolecular helices.

Halogen bonding was further supported by examining in solvents of different alkalinity. On addition of a 20% volume fraction of H₂O into CH₃CN, the CD spectrum of **1L** experiences a significant change and a weakening of the intensity. In contrast, addition of 20% by volume THF, a solvent of weaker electron donating capacity, results in a minor change in the CD spectrum. These observations support the hypothesis that halogen bonding serves as an interaction force between

molecules (Fig. S14–S16, ESI†).[18] Cl⁻, Br⁻, and I⁻ anions can act as halogen bond receptors, and their ability to destroy halogen bonds follows the order of I⁻ > Br⁻ > Cl⁻.[19] On addition of halogen anions at a high concentration of 100 equivalents into CH₃CN solution of **1L**, the CD signal of the supramolecular species of **1L** gradually decreases (Fig. S17, ESI†), and the order of intensity decline is the same as their destructive ability towards halogen bonds, *i.e.*, I⁻ > Br⁻ > Cl⁻ (Fig. S18, ESI†).

NMR spectra also support the existence of intermolecular halogen bonding. In comparison to the ¹H NMR spectrum of monomeric **1L** in pure DMSO-d_6, we observed additional weak ¹H NMR signals of **1L** in CD₃CN/DMSO-d_6 (200 : 1, v/v) (Fig. S19, ESI†), which were assigned to the assembled oligomers, as evidenced by the COSY couplings of H$^{k'}$–H$^{l'}$, H^{f}–H$^{g'}$ and H$^{f'}$–H$^{g'}$ (Fig. S20, ESI†). Interestingly, clear NOESY coupling signals are shown for H^e–H^k, H^e–H^l, H^f–H^k, H^f–H^l and H^j–H^l in CD₃CN/DMSO-d_6 (200 : 1, v/v), but no such couplings are observed in DMSO-d_6 at the same concentration. According to the calculated structure of monomeric **1L**, pairs of protons H^e–H^k, H^e–H^l, H^f–H^k, and H^f–H^l are too far apart to be intramolecularly coupled. Only when the intermolecular C–I···O bonds link adjacent **1L** molecules, benzene ring **C** in which H^k and H^l are located will be brought into close proximity to benzene ring **A** from another **1L** molecule that contains H^e and H^f, resulting in clear intermolecular coupling signals (Fig. S21, ESI†). We thus proposed that the formation of supramolecular assemblies of **1L** is driven by intermolecular C–I···O halogen bonding.

In **1L**, the β-turn provides the helical conformation, four of which are spaced by *meta*-substituted benzene rings, which is more conducive to the propagation of the helicity of the turn structure. We thus developed control compounds **3L**, **4L** and **5L**, containing, respectively, 1, 2, and 3 *para*-substituted benzene spacers (Fig. 1b). CD spectra in CH₃CN show that these three control compounds exhibit weaker CD intensities than **1**, and the signal peaks appear at shorter wavelengths (Fig. S22, ESI†). The g factor values of **3L**, **4L**, and **5L** are significantly smaller than that of **1L** (Fig. 4a). This finding further supports the superior propagation of the helicity of **1L** and highlights the synergy of the *meta*-substitution at the benzene spacers in facilitating the transmission of homochirality. In addition, we compared the spectra of the control compounds containing different numbers of β-turns, **6L** containing only one and **7L** containing two (Fig. 1b). The CD spectra show that at the same concentration of the β-turn in **1L**, **6L**, and **7L**, **1L** in CH₃CN exhibits a much higher CD intensity and a larger g factor than those of **6L** and **7L** (Fig. 4a and Fig. S23, ESI†). Even at increased concentrations of 60 μM for **6L** and 200 μM for **7L**, no assembly was observed (Fig. S24 and S25, ESI†). This suggests that the size of the oligomeric building block is important too, and smaller does not guarantee a stronger tendency of assembly, despite being less flexible. In view of the SEM images, none of the control compounds (**2L**, **3L**, **4L**, **5L**, **6L** and **7L**) were found to assemble into helical aggregates in CH₃CN (Fig. S26, ESI†). It is of interest to recall that the *para*-substituted benzene spaced
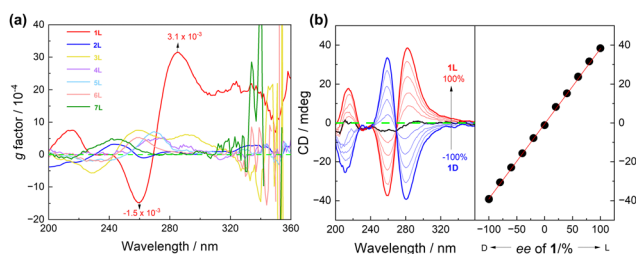

Fig. 4 (a) Wavelength profiles of the g factors of **1L–7L** in CH₃CN. [**1L–5L**] = 10 μM, [**6L**] = 40 μM, and [**7L**] = 20 μM. (b) CD spectra of mixtures of **1L** and **1D** of various *ee* in CH₃CN and plots of the CD signals at 281 nm against *ee*. [**1L**] + [**1D**] = 10 μM.

counterpart of **7L** containing two β-turns undergoes assembly into helices in dilute CH_3CN,[15] again highlighting the critical role of the spacer that links the β-turn structures.

Temperature-dependent CD signals of **1L** in CH_3CN show that the helix is highly heat stable. The CD intensity was only slightly reduced upon heating the solution up to 70 °C and it can be completely restored after cooling (Fig. S27 and S28, ESI†). The enantiomeric mixtures of **1L** and **1D** of varying ratios in CH_3CN show a linear-dependence of the CD signals on the enantiomeric excess (*ee*) (Fig. 4b), suggesting that the enantiomers of **1L** and **1D** are self-sorting in their assemblies.[20,21] This is different from the single-stranded helix from the building blocks *via* C–I···π halogen bonding (S-shaped CD-*ee* dependence),[15] but similar to that of the double helix driven by two crossed C–I···S halogen bonds.[16]

In summary, an oligomeric building block that contains four β-turns using a benzoylalanine-based amidothiourea motif is shown to be of optimal minimum length to allow efficient assembly into a supramolecular helix. **1L** or **1D** in which four β-turn structures are spaced by *meta*-substituted benzene rings undergoes assembly in CH_3CN at a μM-level concentration, *via* intermolecular halogen bonding. The formed helix exhibits strong CD signals of a high *g* factor of 3.1×10^{-3} at 285 nm for instance and a linear CD-*ee* dependence, together with an excellent thermal stability. DLS data show that the length of the formed supramolecular helix is finite. Replacing the *meta*-substituted benzene spacers with *para*-substituted one(s) substantially decreases the tendency of assembling, highlighting the critical role of helicity propagation in facilitating the helical assembly, and neither does a decrease in the number of β-turns spaced by *meta*-substituted benzenes. We therefore show that with oligomeric helical building blocks, an optimal number of turns and the way they are spaced are important factors dictating their assembly into helices.

Conflicts of interest

The authors declare no conflicts of interest.

Notes and references

1 C. Z. Liu, M. Yan, H. Wang, D. W. Zhang and Z. T. Li, *ACS Omega*, 2018, **3**, 5165–5176.
2 E. Yashima, N. Ousaka, D. Taura, K. Shimomura, T. Ikai and K. Maeda, *Chem. Rev.*, 2016, **116**, 13752–13990.
3 M. Gonzalez-Sanchez, M. J. Mayoral, V. Vazquez-Gonzalez, M. Paloncyova, I. Sancho-Casado, F. Aparicio, A. de Juan, G. Longhi, P. Norman, M. Linares and D. Gonzalez-Rodriguez, *J. Am. Chem. Soc.*, 2023, **145**, 17805–17818.
4 Q. Gan, Y. Wang and H. Jiang, *Chin. J. Chem.*, 2013, **31**, 651–656.
5 D. J. Hill, M. J. Mio, R. B. Prince, T. S. Hughes and J. S. Moore, *Chem. Rev.*, 2001, **101**, 3893–4012.
6 H. Juwarker, J. M. Suk and K. S. Jeong, *Chem. Soc. Rev.*, 2009, **38**, 3316–3325.
7 D. W. Zhang, X. Zhao, J. L. Hou and Z. T. Li, *Chem. Rev.*, 2012, **112**, 5271–5316.
8 D. W. Zhang, W. K. Wang and Z. T. Li, *Chem. Rec.*, 2015, **15**, 233–251.
9 C. Z. Liu, S. Koppireddi, H. Wang, D. W. Zhang and Z. T. Li, *Angew. Chem., Int. Ed.*, 2019, **58**, 226–230.
10 T. Yan, F. Yang, S. Qi, X. Fan, S. Liu, N. Ma, Q. Luo, Z. Dong and J. Liu, *Chem. Commun.*, 2019, **55**, 2509–2512.
11 Y. Ferrand and I. Huc, *Acc. Chem. Res.*, 2018, **51**, 970–977.
12 C. Zhang, X. Deng, C. Wang, C. Bao, B. Yang, H. Zhang, S. Qi and Z. Dong, *Chem. Sci.*, 2019, **10**, 8648–8653.
13 X. Yan, P. Weng, D. Shi and Y.-B. Jiang, *Chem. Commun.*, 2021, **57**, 12562–12574.
14 D. Bindl, P. K. Mandal and I. Huc, *Chem. – Eur. J.*, 2022, **28**, e202200538.
15 J. Cao, X. Yan, W. He, X. Li, Z. Li, Y. Mo, M. Liu and Y.-B. Jiang, *J. Am. Chem. Soc.*, 2017, **139**, 6605–6610.
16 X. Yan, K. Zou, J. Cao, X. Li, Z. Zhao, Z. Li, A. Wu, W. Liang, Y. Mo and Y.-B. Jiang, *Nat. Commun.*, 2019, **10**, 3610.
17 M. M. Smulders, M. M. Nieuwenhuizen, T. F. de Greef, P. van der Schoot, A. P. Schenning and E. W. Meijer, *Chem. – Eur. J.*, 2010, **16**, 362–367.
18 C. Laurence, M. Queignec-Cabanetos, T. Dziembowska, R. Queignec and B. Wojtkowiak, *J. Am. Chem. Soc.*, 2002, **103**, 2567–2573.
19 A. Mele, P. Metrangolo, H. Neukirch, T. Pilati and G. Resnati, *J. Am. Chem. Soc.*, 2005, **127**, 14972–14973.
20 X. Yan, Q. Wang, X. Chen and Y.-B. Jiang, *Adv. Mater.*, 2020, **32**, e1905667.
21 C. Roche, H. J. Sun, M. E. Prendergast, P. Leowanawat, B. E. Partridge, P. A. Heiney, F. Araoka, R. Graf, H. W. Spiess, X. Zeng, G. Ungar and V. Percec, *J. Am. Chem. Soc.*, 2014, **136**, 7169–7185.